Available online at www.sciencedirect.com
SCIENCE DIRECT®
Journal of Sound and Vibration 276 (2004) 729–754
JOURNAL OF SOUND AND VIBRATION
www.elsevier.com/locate/jsvi

On the limits of an "in vacuum" model to determine the mechanical parameters of isotropic poroelastic materials

O. Danilov, F. Sgard*, X. Olny

Lab. des Sciences de l'Habitat, Dep. Genie Civil et Batiment, Ecole Nationale des Travaux Publics de l'Etat, URA CNRS 1652, Rue Maurice Audin, Vaulx-en-Velin, Cedex 69518, France

Received 4 October 2002; accepted 5 August 2003

Abstract

The prediction of the acoustic performance of multi-layered structures involving porous materials now classically relies on the use of Biot's theory for the modelling of the porous medium. In particular, it is of prime importance to correctly assess the mechanical parameters of the porous skeleton "in vacuum". However, measurements of these parameters "in vacuum" conditions comprises some problems so that they are commonly carried out in ambient conditions assuming that the response of the porous material is not influenced by its fluid phase and solely determined by the parameters of its solid phase. The purpose of this work is to investigate the conditions when a mechanically excited porous material exhibits indeed an "in vacuum" behaviour. The comparison between the air-saturated and the "in vacuum" models is carried out both in the case of impedance infinite models and taking into account finite lateral dimensions of the porous sample. It is shown that a model accounting for finite dimensions of the porous samples must be considered in order that Biot's and "in vacuum" models yield identical mechanical responses. More precisely, a "poroelastic" shape factor defined as the ratio of the volume of the porous sample to the area of its free lateral sides is introduced to quantify the mismatch between the two models. For small values of this parameter, the mechanical response of the porous material calculated using Biot's model is similar to the one predicted using the "in vacuum" model. For higher values, the responses calculated by the two models exhibit noticeable differences. The corresponding limiting value of the poroelastic shape factor is shown to depend on the flow resistivity together with the thickness of the porous sample.

1. Introduction

Porous materials are widely used as passive elements involved in noise reduction systems. They are often employed in automotive, aircraft, building and several other industries. Currently, each

*Corresponding author. Fax: +33-4-72-04-70-41.
E-mail address: franck.sgard@entpe.fr (F. Sgard).

0022-460X/$ - see front matter © 2003 Elsevier Ltd. All rights reserved.
doi:10.1016/j.jsv.2003.08.036

industrial solution requires a deep engineering working, which always includes the prediction of the efficiency of this solution. Finite-element methods are an efficient tool to simulate transmission loss, sound absorption efficiency and damping properties of porous materials at low frequencies [1–5]. Biot's model is commonly used in finite-element formulation of porous layers. This model requires a correct assessment of the material parameters. The acoustical parameters, such as porosity, flow resistivity, geometrical tortuosity, viscous and thermal characteristic lengths can be determined by direct [6] or indirect methods [7,8]. Other important characteristics of porous material parameters are the mechanical ones, which include complex Young's modulus and the Poisson ratio. The goal of this paper is to discuss some limitations of the measurement of the mechanical parameters of isotropic porous media via dynamic compression tests. Several other methods allowing for an extraction of the mechanical parameters of porous media are available but they will not be considered here. One can mention for instance the identification of these parameters from an analysis of pseudo-Rayleigh waves [9], from measurements of the vibration behaviour of a plate coupled with the porous layer [10] or from transmission loss measurements [11].

Currently, two principal types of dynamic compression test methods are used for E-modulus measurements. Both types utilize mechanical excitation of the porous medium and are used in the low-frequency range. The first category referred to as resonances methods (or transfer function methods) allows for an estimation of the mechanical parameters at discrete frequencies (resonance frequencies). In this case the porous layer combined with an additional mass is assumed to behave as a mass–spring system [12,13], and the complex Young's modulus is determined by the parameters of the resonance (resonance frequency, thickness of resonance curve). Also, there are techniques based on the resonance behaviour, which provide a continuous dependency of Young's modulus on the frequency [14]. The second category referred to as non-resonances methods, among which the ones called "direct dynamic", or "quasi-static" if they operate in the low-frequency range, yields a continuous dependency of mechanical parameters on the frequency [15,16]. These methods comprise some difficulties related, for example, to the necessity of an additional static load. Both types of measurement methods rely on the same assumptions, e.g., the fluid phase of the porous material is usually assumed to play a negligible role in the low-frequency range [15] (typically frequencies below 50 Hz) so that the material can be considered in "in vacuum" conditions [15]. In this case, it is only described by the characteristics of its skeleton, namely by complex Young's modulus, the Poisson ratio, and density. Although Biot's model uses mechanical parameters of the porous skeleton "in vacuum", a real measurement of these parameters "in vacuum" induces some problems, e.g., the reduction of temperature of the porous frame in vacuum, which changes the properties of the frame. Moreover, there are some types of foams, the skeleton of which can be completely destroyed under vacuum conditions. In order to avoid these issues, experimenters carry out the measurements of mechanical Biot's parameters under ambient conditions and considering the porous medium as a viscoelastic material.

Thus, it is of prime importance to compare the "in vacuum" and poroelastic descriptions of a porous material. Taking into account that the parameters of the porous medium are determined as input data to numerical prediction tools, the goal of this work is to examine analytically the conditions and limits, for which air-saturated porous materials described by a complete Biot's model and an "in vacuum" model behave in the same way.

The paper is organized as follows. To compare the poroelastic and "in vacuum" models of a porous medium, the equations of the impedance of a structure classically used for measurement of mechanical parameters are established. Normally, this structure consists of the porous medium backed by a hard wall and mechanically excited. This mechanical excitation is simulated by an oscillating impervious lightweight screen, which transfers the mechanical excitation to the skeleton of the porous material. Then, the same system is analyzed in the case of a porous sample with finite lateral dimensions and with a mass atop (such a structure is also widely used for measurements of mechanical parameters). The conditions, which influence the "in vacuum" and poroelastic behaviours of the porous material, such as the sample dimensions and frequency range, are examined.

2. Theory

Considering the measurement systems intended for the determination of the mechanical parameters of porous materials (see Fig. 1), one can observe several common elements for all existing set-ups. In the case of transfer function methods (one type of resonance method), the porous material is placed between a vibrating base (1) and an additional mass (3), see Fig. 1(a). In the case of resonance methods with excitation through mass by non-contact excitation (5), it is located between a motionless rigid frame (4) and an additional mass (3), see Fig. 1(b). And finally, in the case of a direct dynamic method, the porous sample is placed between a motionless frame (4) and a vibrating base (1), (Fig. 1(c)). Thus, all the methods rely on a mechanical excitation of the porous sample, which is placed between two impervious screens, and two methods suppose an additional mass atop the porous layer. Therefore, to compare the behaviours of Biot's and "in vacuum" models of the porous material, it is necessary to present the analytical equations for the impedance of a porous and an "in vacuum" layer backed by a rigid wall, covered by an additional mass and excited mechanically.

2.1. Displacement excitation of an air-saturated porous material backed by an impervious rigid wall

First, consider the determination of the impedance of an air-saturated porous sample excited mechanically.

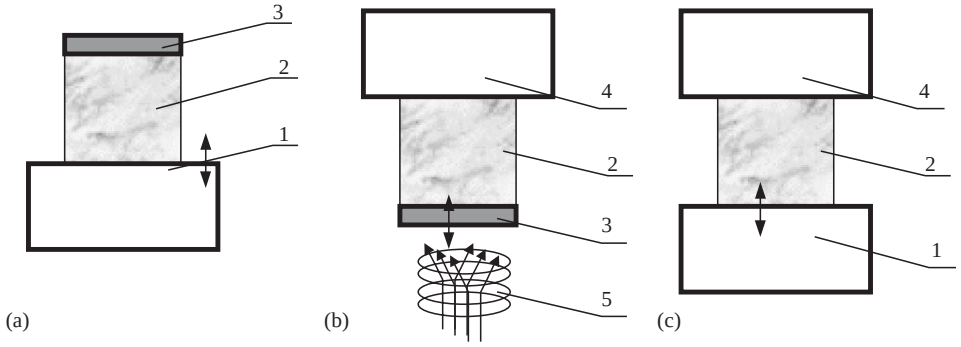

Fig. 1. Principal types of measurements set-ups.

Physically, such type of excitation can be observed in the case of a light-weight impervious screen attached to the porous layer. This screen represents a field of displacements acting onto the porous material by transferring the stresses and velocities to the frame and to the air in the material. The excitation is applied in the normal direction to the surface of porous layer. The normal direction of excitation means an absence of Biot's shear wave. Thus, according to Biot's theory, two incident and two reflected compressional waves should propagate in the direction normal to the rigid wall. The derivation of the characteristic impedance is inspired by Ref. [17] for a normal incidence plane wave. The difference is just in the type of excitation to which the porous material is submitted, that is velocity instead of pressure. Fig. 2 shows the porous material backed by the rigid wall and excited normally to its surface. The x-component of the total stress vector acting on the porous material is given by

$$\sigma_{xx}^{tot}(x) = -Z_c V(x), \tag{1}$$

where Z_c is the characteristic impedance of the structure and V denotes the total velocity of the porous material (or the velocity of the impervious screen).

Fig. 2 shows the incident and reflected waves (indexes i and r) and normal stresses in the material (superscripts s and f refer to solid and fluid). For all the fields a $e^{j\omega t}$ temporal dependency is assumed.

If x denotes the direction of wave propagation, the stresses in the porous material, the normal velocities of the frame $\dot{u}^s$ and the velocity of the air in the pores $\dot{u}^f$ are given by [17]

$$\sigma_{xx}^s = -Z_1^s(V_1^i e^{-j\delta_1 x} - V_1^r e^{j\delta_1 x}) - Z_2^s(V_2^i e^{-j\delta_2 x} - V_2^r e^{j\delta_2 x}), \tag{2}$$

$$\sigma_{xx}^f = -\phi Z_1^f \mu_1(V_1^i e^{-j\delta_1 x} - V_1^r e^{-j\delta_1 x}) - \phi Z_2^f \mu_2(V_2^i e^{-j\delta_2 x} - V_2^r e^{-j\delta_2 x}), \tag{3}$$

$$\dot{u}^s = (V_1^i e^{-j\delta_1 x} + V_1^r e^{j\delta_1 x}) + (V_2^i e^{-j\delta_2 x} + V_2^r e^{j\delta_2 x}), \tag{4}$$

$$\dot{u}^f = \mu_1(V_1^i e^{-j\delta_1 x} + V_1^r e^{j\delta_1 x}) + \mu_2(V_2^i e^{-j\delta_2 x} + V_2^r e^{j\delta_2 x}), \tag{5}$$

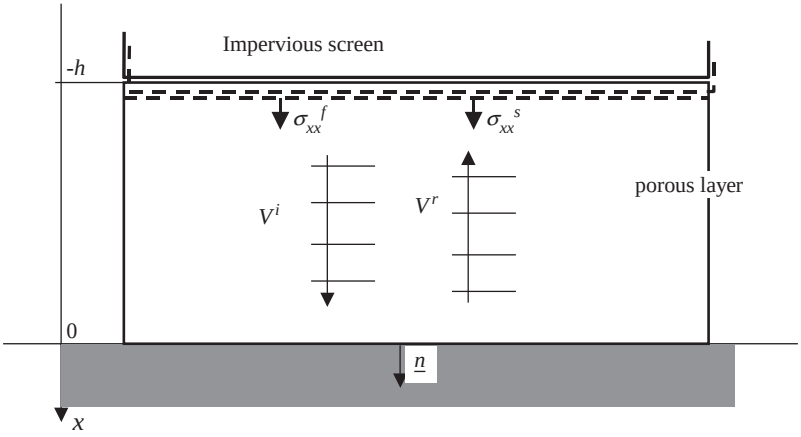

Fig. 2. Impervious screen coupled to a porous layer backed by a rigid wall.

where Z_1^s, Z_2^s, Z_1^f and Z_2^f are the characteristic impedances of the solid phase and the fluid phase determined by [17]

$$Z_1^S = (P + Q\mu_1)\frac{\delta_1}{\omega}, \tag{6}$$

$$Z_2^S = (P + Q\mu_2)\frac{\delta_2}{\omega}, \tag{7}$$

$$Z_1^f = (R + (\tfrac{Q}{\mu_1}))\frac{\delta_1}{\phi\omega}, \tag{8}$$

$$Z_2^f = (R + (\tfrac{Q}{\mu_2}))\frac{\delta_2}{\phi\omega}, \tag{9}$$

δ_1, δ_2 are the wavenumbers of Biot's compressional waves, determined by equations

$$\delta_1^2 = \frac{\omega^2}{2(PR - Q^2)}[P\tilde{\rho}_{22} + R\tilde{\rho}_{11} - 2Q\tilde{\rho}_{12} - \sqrt{\Delta}], \tag{10}$$

$$\delta_2^2 = \frac{\omega^2}{2(PR - Q^2)}[P\tilde{\rho}_{22} + R\tilde{\rho}_{11} - 2Q\tilde{\rho}_{12} + \sqrt{\Delta}], \tag{11}$$

where Δ is given by

$$\Delta = (P\tilde{\rho}_{22} + R\tilde{\rho}_{11} - 2Q\tilde{\rho}_{12})^2 - 4(PR - Q^2)(\tilde{\rho}_{11}\tilde{\rho}_{22} - \tilde{\rho}_{12}^2), \tag{12}$$

μ_1, μ_2 are given by [17]

$$\mu_i = \frac{(P\delta_i^2 - \omega^2\tilde{\rho}_{11})}{(\omega^2\tilde{\rho}_{12} - Q\delta_i^2)}, \quad i = 1, 2, \tag{13}$$

ϕ is the porosity of the porous material.

The poroelastic coefficients (P, Q, R) are expressed as

$$P = \frac{4}{3}N + K_b + \frac{(1-\phi)^2}{\phi}K_f, \tag{14}$$

$$Q = K_f(1 - \phi), \tag{15}$$

$$R = \phi K_f, \tag{16}$$

where N is the shear modulus of the frame, K_b is the bulk modulus of the frame, and K_f is the bulk modulus of the fluid inside the porous material.

The effective Biot's densities ($\tilde{\rho}_{11}$, $\tilde{\rho}_{12}$, $\tilde{\rho}_{22}$) see Ref. [17], are

$$\tilde{\rho}_{11} = \rho_1 + \rho_a - \mathrm{j}\sigma\phi^2\frac{G(\omega)}{\omega}, \tag{17}$$

$$\tilde{\rho}_{12} = -\rho_a + \mathrm{j}\sigma\phi^2\frac{G(\omega)}{\omega}, \tag{18}$$

$$\tilde{\rho}_{22} = \phi\rho_0 + \rho_a - \mathrm{j}\sigma\phi^2\frac{G(\omega)}{\omega}, \tag{19}$$

where ρ_1 is the density of the frame, ρ_0 is the density of the air, σ is the flow resistivity of the porous material. The quantities ρ_a and $G(\omega)$ are given by

$$\rho_a = \rho_0 \phi(\alpha_\infty - 1), \tag{20}$$

$$G(\omega) = \sqrt{1 + \frac{4j\alpha_\infty^2 \eta \rho_0 \omega}{\sigma^2 \Lambda^2 \phi^2}}, \tag{21}$$

where α_∞ is the geometrical tortuosity, η is the viscosity of the interstitial fluid, and Λ is the viscous characteristic length determined by

$$\Lambda = \sqrt{\frac{4\alpha_\infty \eta}{\sigma \phi}}. \tag{22}$$

Thus, having the equations of the stresses and velocities (Eqs. (2)–(5)), one can then consider the boundary conditions (see Fig. 2). At the rigid wall ($x = 0$) the latter read $\dot{u}^f(0) = \dot{u}^s(0) = 0$, which leads to

$$V_1^i = -V_1^r \quad \text{and} \quad V_2^i = -V_2^r, \tag{23}$$

At $x = -t$, the impervious screen is attached to the porous layer and boundary conditions are given by (taking into account the nullity of the normal flux and the continuity of the solid and screen displacements at the screen–porous interface):

$$\dot{\mathbf{u}}^m = (1 - \phi)\dot{\mathbf{u}}^s + \phi \dot{\mathbf{u}}^f, \tag{24}$$

$$\phi(\dot{\mathbf{u}}^s - \dot{\mathbf{u}}^f) \cdot \mathbf{n} = 0, \tag{25}$$

where $\mathbf{n}$ denotes the outward normal to the surface and $\dot{u}^m = \dot{\mathbf{u}}^m \cdot \mathbf{n}$ refers to the screen velocity.

The combination of Eqs. (24) and (25) leads to

$$\dot{u}^m = \mathbf{n} \cdot \dot{\mathbf{u}}^s, \tag{26}$$

and to

$$\dot{u}^m = \dot{u}^s = \dot{u}^f \quad \text{at } x = -t \tag{27}$$

The total stress ($\sigma_{xx}^{tot} = \sigma^{tot}.\mathbf{n}$) in the porous material at $x = -t$ (normal to the interface) is related to the normal force applied by the screen onto the porous sample and the corresponding excitation area S:

$$\sigma_{xx}^{tot} = -\frac{F}{S}, \tag{28}$$

Force F can also be written as

$$F = Z_{mech} \dot{u}^m, \tag{29}$$

where Z_{mech} is the mechanical impedance of the porous layer, ($Z_{mech} = Z_c S$). The total stress is given by

$$\sigma_{xx}^{tot} = \sigma_{xx}^{s} + \sigma_{xx}^{f}, \tag{30}$$

and Eqs. (28) and (29) lead to

$$\sigma_{xx}^{tot} = -\frac{Z_{mech}\dot{u}^m}{S}, \tag{31}$$

Recalling Eqs. (2) and (3), the total stress in the porous layer can be expressed as a function of characteristic impedances of Biot's compressional waves:

$$\sigma_{xx}^{tot} = -\dot{u}^m Z_c = -2(Z_1^s + \mu_1 Z_1^f)\cos(\delta_1 l)V_1^i - 2(Z_2^s + \mu_2 Z_2^f)\cos(\delta_2 l)V_2^i. \tag{32}$$

In addition, Eqs. (4) and (5) can be rewritten as

$$\dot{u}^m = 2\mathrm{j}\sin(\delta_1 l)V_1^i + 2\mathrm{j}\sin(\delta_2 l)V_2^i, \tag{33}$$

$$\dot{u}^m = 2\mathrm{j}\mu_1\sin(\delta_1 l)V_1^i + 2\mathrm{j}\mu_2\sin(\delta_2 l)V_2^i. \tag{34}$$

The system of Eqs. (32)–(34) is an homogeneous system which has a non-trivial solution ($\dot{u}^m$, V_1^i, V_2^i) if

$$\begin{vmatrix} Z_c & -2(Z_1^s + \mu_1 Z_1^f)\cos(\delta_1 l) & -2(Z_2^s + \mu_2 Z_2^f)\cos(\delta_2 l) \\ 1 & -2j\sin(\delta_1 l) & -2j\sin(\delta_2 l) \\ 1 & -2j\mu_1\sin(\delta_1 l) & -2j\mu_2\sin(\delta_2 l) \end{vmatrix} = 0, \tag{35}$$

that is, if

$$Z_c = j\frac{[(Z_2^s + \mu_2 Z_2^f)\cot(\delta_2 l)(1-\mu_1) - (Z_1^s + \mu_1 Z_1^f)\cot(\delta_1 l)(1-\mu_2)]}{(\mu_1 - \mu_2)}. \tag{36}$$

Thus, Eq. (37) allows one to calculate the characteristic impedance of the porous layer backed by a rigid wall and excited mechanically.

2.2. Displacement (velocity) excitation of a porous material backed by an impervious rigid wall in vacuum

The porous material is now considered to be "in vacuum". In general, the material in this situation can be considered as a homogenous viscoelastic one, but one could find it interesting to derive an impedance equation starting from Biot's model. Thus, the porous material "in vacuum" is characterized by the absence of air in the pores, and for a normal excitation, only one compressional wave propagates in the frame. So, the equation of motion for the solid phase is classically given by Allard [17].

$$\nabla^2\varphi^s + \omega^2\frac{\tilde{\rho}_{11}}{P}\varphi^s = 0, \tag{37}$$

where $\tilde{\rho}_{11}$ is the dynamic density of the solid frame. In the case of a vacuum it reduces to the density of the solid frame.

φ^s is a scalar potential, such that $\mathbf{u}^s = \nabla\varphi^s$ with

$$\delta^2 = \omega^2\frac{\tilde{\rho}_{11}}{P}, \tag{38}$$

where the elastic coefficient P reduces to [17]

$$P = \frac{4}{3}N + K_b = \frac{2N(1-v)}{(1-2v)}. \tag{39}$$

In Eq. (39), N denotes the shear modulus, $K_b = [2N(v+1)/3(1-2v)]$, and v is the Poisson ratio.

The characteristic impedance of the compressional wave in vacuum condition ($Q = 0$) is then given by

$$Z^s = P\frac{\delta}{\omega} = \sqrt{\tilde{\rho}_{11}P}. \tag{40}$$

The mechanical impedance of the porous layer in vacuum can be obtained from the stress tensor σ^s_{xx} and the skeleton velocity $\dot{u}^s$:

$$\sigma^s_{xx} = -Z^s(V^i e^{-j\delta x} - V^r e^{j\delta x}), \tag{41}$$

$$\dot{u}^s = (V^i e^{-j\delta x} + V^r e^{j\delta x}). \tag{42}$$

Considering boundary conditions $\dot{u}^s(0) = 0$ and $\dot{u}^m = \dot{u}^s(-t)$, the mechanical impedance reads

$$Z_{mech} = \frac{F}{\dot{u}^m} = \frac{\sigma^s_{xx}(-t)S}{\dot{u}^s(-t)} = \frac{-2jZ^s\dot{u}^m S\sin(\delta t)}{2\dot{u}^m\cos(\delta t)} = -j\frac{Z^s S}{\tan(\delta t)}. \tag{43}$$

Using the relation $Z_{mech} = Z_{c,vac}S$, the characteristic impedance of the porous layer in vacuum $Z_{c,vac}$ reads

$$Z_{c,vac} = -j\frac{Z^s}{\tan(\delta t)}. \tag{44}$$

2.3. Behaviour of a porous material with a mass ontop

Taking into account that the system consisting of a porous layer backed by an impervious rigid wall and covered by an additional mass is frequently used as a resonance measurement system, such a system can also be analyzed.

The total mechanical impedance of the system shown in Figs. 1(a) and (b) in the case of its excitation through the mass is given by

$$\frac{F}{\dot{x}} = Z_{mec,tot} = Z_m + Z_p, \tag{45}$$

where $\dot{x}$ is the mass velocity, F is the exciting force, $Z_{mec,tot}$ is the mechanical impedance of the total system, Z_m is the impedance of additional mass, $Z_m = j\omega M_{add}$, where M_{add} refers to as an added mass, Z_p is the mechanical impedance of the porous sample. Note that $Z_p = Z_{mech}$ for "in vacuum" conditions, where Z_{mech} is determined by Eq. (43). $Z_p = Z_c S$ in the case of air-saturated porous material, where Z_c is determined by Eq. (36), and S is the contact area between the mass and the porous material.

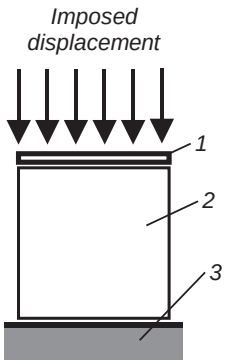

Fig. 3. Schema of finite-element resonant oscillating system.

2.4. Finite-element model of the porous material

The prediction of the behaviour of a finite-dimension porous sample requires a numerical description. A finite-element model has been selected here. It is based on the mixed displacement-pressure poroelastic formulation developed by Atalla et al. [5]. The calculations have been performed using a commercial software which relies on this formulation [18]. The finite-dimension porous sample is supposed to be excited in a mechanical way (displacement excitation) using a weightless impervious screen. The chosen structure is depicted in Fig. 3. In this figure, (1) corresponds to the weightless exciting piston, (2) denotes the porous material, and (3) the rigid base. The excitation through a weightless piston is equivalent to an imposed displacement applied on the porous layer. It is supposed that the piston does not influence any parameters of the system, it just transforms a sound pressure into a vibration velocity acting on the porous material.

In the following, when considering the air-saturated model, the porous sample is discretized using linear poroelastic hexahedral eight noded elements with four degrees of freedom per node (three solid displacements, interstitial pressure). The finite-element modelling of the material "in vacuum" utilizes linear "solid" hexahedral eight noded elements. In the configuration of the porous layer with a mass atop, the mass has been discretized with linear septum (surface element without stiffness) four noded elements.

3. Infinite approach: comparison between "air-saturated" and "in vacuum" conditions

The comparisons have first been performed with materials whose acoustic and mechanical parameters have been determined experimentally. In order to cover a large panel of situations corresponding to different behaviours of porous materials, the influence of the skeleton stiffness together with the frequency range where the resonance occurs (medium, low or high) have been investigated by varying Young's modulus or adding a mass atop the porous sample.

The first step of this investigation deals with the comparison of poroelastic and "in vacuum" models in the case of a "fibrous" material (the Poisson ratio is close to 0). The characteristics of this material referred to as material A are presented in Table 1. The comparison between the two models has been carried out in terms of characteristic impedance calculated from Eqs. (36) and

Table 1
Properties of material A

Density (bulk) ρ (kg/m^3)	100
Porosity ϕ	0.985
Flow resistivity σ (Ns/m^4)	46503
Geometrical tortuosity α_∞	1.004
Viscous characteristic length Λ (m)	3.5×10^{-5}
Thermal characteristic length Λ' (m)	4.3×10^{-5}
Young's modulus E (kPa)	170
Loss factor η	0.23
The Poisson ratio ν	0

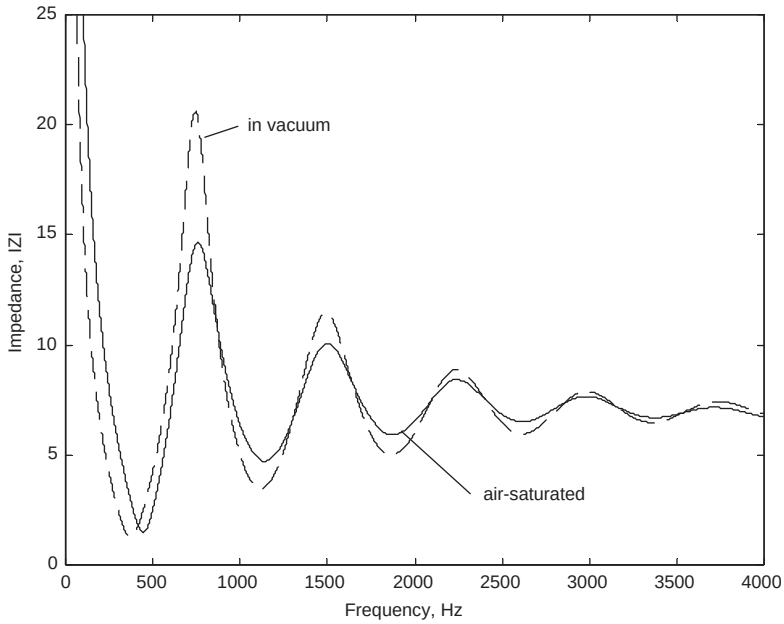

Fig. 4. Modulus of the impedance of porous material A calculated using "air-saturated" and "in vacuum" models.

(44), (see Fig. 4). The resonances of the material "in vacuum" (solid part), corresponding to the minima of impedance curves are clearly seen. In the case of the material "in vacuum", these frequencies correspond to $\frac{1}{4}$ of wavelength resonance of skeleton given by

$$f_{res} = \frac{n}{4t}\sqrt{\frac{P}{\tilde{\rho}_{11}}}, \quad n = 1, 2, 3\ldots . \tag{46}$$

Fig. 4 exhibits differences between the two models in terms of amplitude and position of the resonance frequencies. Note that there is a mismatch between resonance frequencies of the air-saturated and "in vacuum" models. This effect is shown more clearly seen in Fig. 5, which

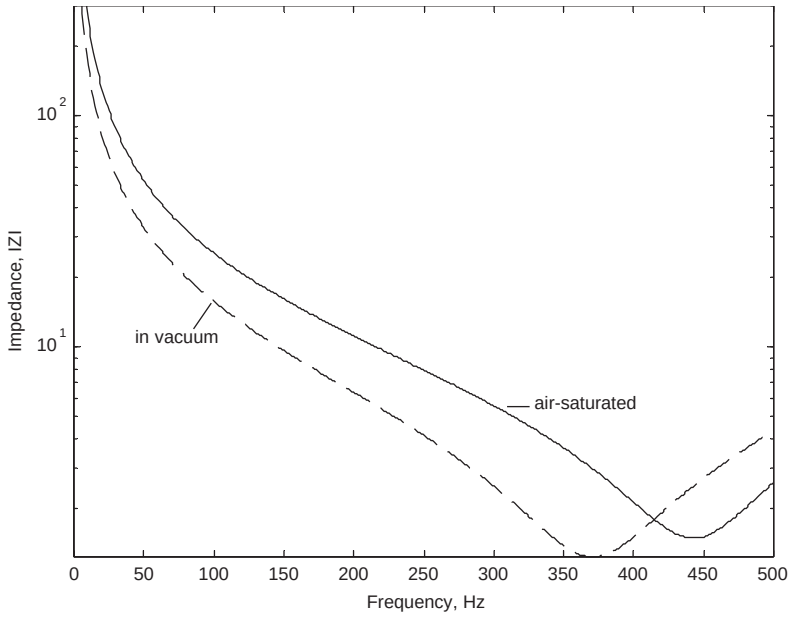

Fig. 5. Modulus of the impedance of porous material A calculated using "air-saturated" and "in vacuum" models.

presents a zoom of Fig. 4 in the frequency range of the first resonance. Next simulation has been made to estimate the effect of increasing Young's modulus on the behaviour of the impedance curves. Fig. 6 displays the impedance moduli calculated respectively with a value of Young's modulus 170 kPa (a) and 600 kPa (b). It is seen that the difference between the impedance of air-saturated material and "in vacuum" material reduces with increasing Young's modulus. Thus, if the skeleton of porous material becomes stiffer, the influence of the air's stiffness on the total stiffness of the material decreases. However, even in the stiffer case (600 kPa) discrepancies occur between the two impedance curves. Similar trends are observed in the case of a foamed porous material (see Fig. 7), whose characteristics are displayed in Table 2. Finally, Fig. 8 displays the moduli of the impedance of material A in the case of a high Young's modulus (5000 kPa). It is seen that the impedance of the air-saturated material is very similar to the "in vacuum" one, but it is important to highlight that this magnitude is unrealistic for porous materials used for acoustic purposes and described by Biot's model.

The next step of the study is to observe the behaviour of the material in the low-frequency range, in the case of low-frequency resonance. There are several possibilities to obtain a low-frequency resonance (in the case of realistic characteristics of porous material), such as the increase of the thickness of the sample, and the decrease (realistically) of Young's modulus of the porous material. In order to avoid unrealistic low values of Young's modulus, a good way is also to use a system made up of a porous material with a mass atop. Moreover, one can recall that this set-up is the typical structure for resonance measurement, as it is shown in Fig. 1. Taking into account that resonance is characterized by an increase of amplitude, the following results are presented in terms of admittance (A), defined as the inverse of impedance, $A = 1/Z$. Fig. 9 shows the admittance calculated for a sample of thickness 28 mm and made up of material A. The Young modulus was reduced to 40 kPa (a) and 80 kPa (b), with a mass atop equal to 0.020 kg. It is seen

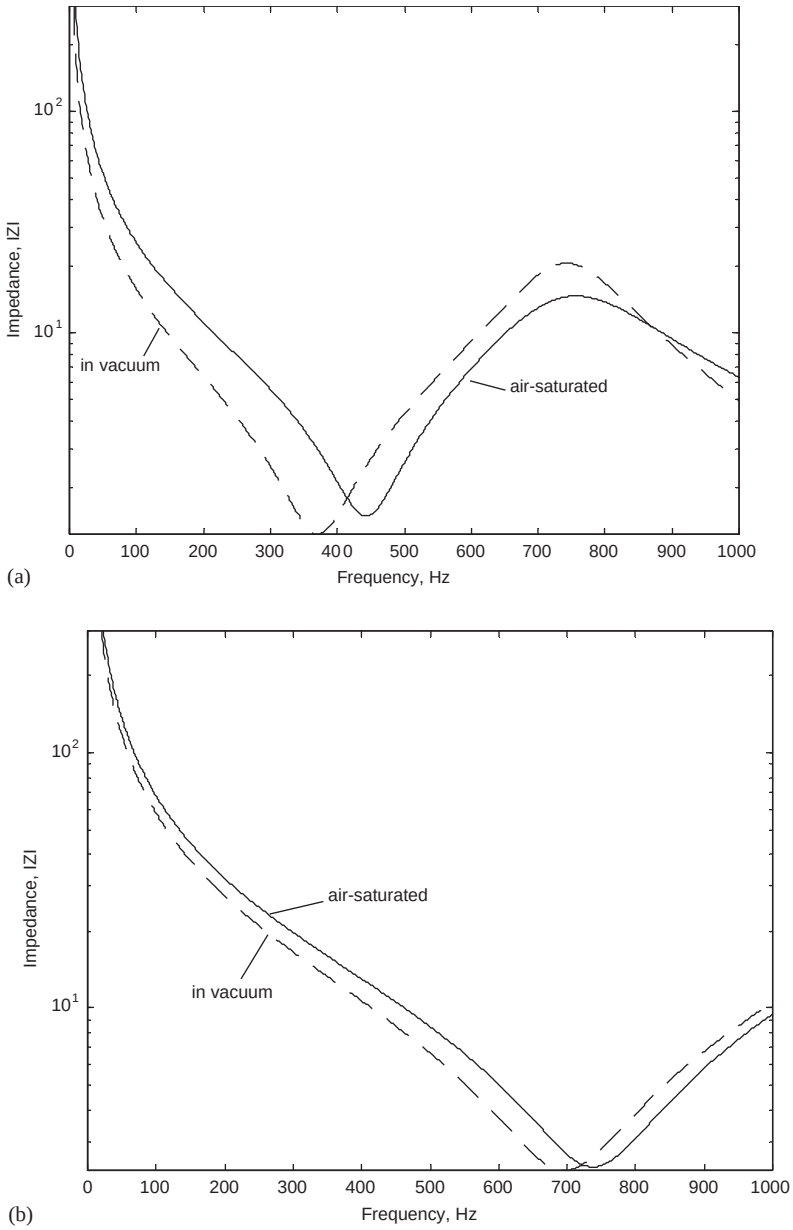

Fig. 6. Modulus of the impedance of porous material A obtained for two values of Young's modulus (a) $E = 170\,\text{kPa}$, (b) $E = 600\,\text{kPa}$ and calculated using "air-saturated" and "in vacuum" models.

that Biot's air-saturated model exhibits a very different behaviour from the "in vacuum" model. The resonance frequencies observed are located between 50 and 120 Hz.

The further reduction of the resonant frequency of the system obtained by increasing the thickness of porous layer to 100 and 200 mm also does not reveal any coincidence between

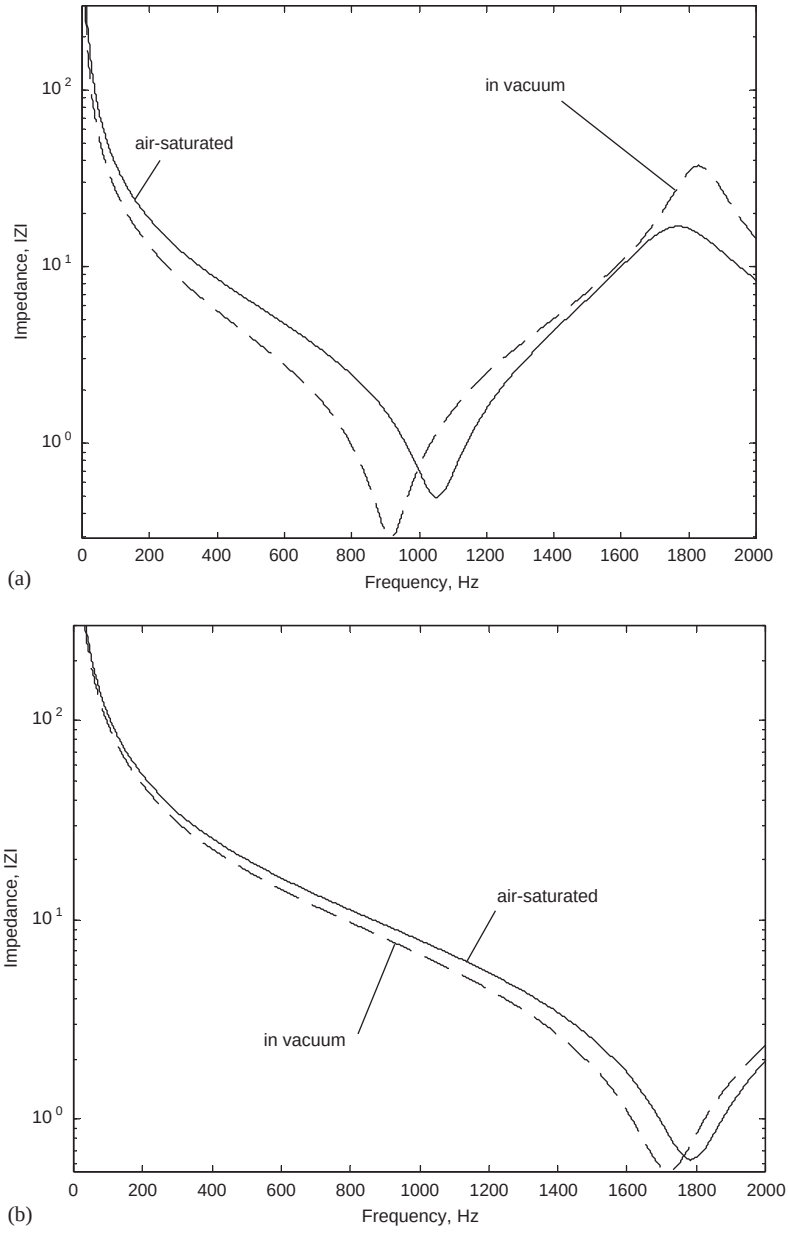

Fig. 7. Modulus of the impedance of porous material A obtained for two values of Young's modulus, (a) $E = 170\,\text{kPa}$, $\nu = 0.35$, (b) $E = 600\,\text{kPa}$, $\nu = 0.35$ and calculated using "air-saturated" and "in vacuum" models.

"in vacuum" and poroelastic models, see Figs. 10a and b. The resonance has been obtained around 50 Hz, and the difference between resonance frequencies in both "in vacuum" and poroelastic models is approximately 10 Hz. Therefore, no agreement was obtained between the dynamic behaviours of "air-saturated" and "in vacuum" conditions in the low-frequency range.

Table 2
Properties of material B

Density (bulk) ρ (kg/m^3)	28
Porosity ϕ	0.975
Flow resistivity σ (Ns/m^4)	13904
Geometrical tortuosity α_∞	1.648
Viscous characteristic length Λ (m)	7.7×10^{-5}
Thermal characteristic length Λ' (m)	26.0×10^{-5}
Young's modulus E (kPa)	170
Loss factor η	0.08
The Poisson ratio v	0.35

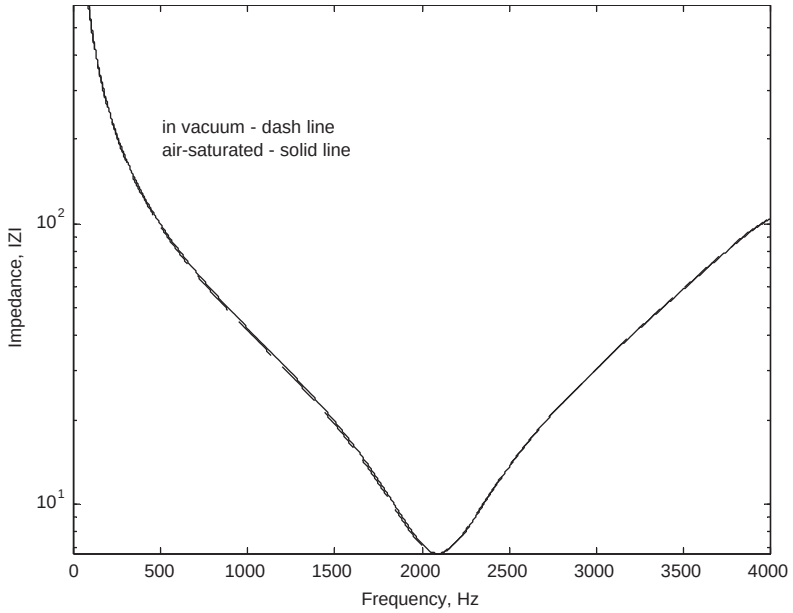

Fig. 8. Modulus of the impedance of porous material A obtained for a high value of Young's modulus ($E = 5000$ kPa) and calculated using "air-saturated" and "in vacuum" models.

Previous results indicated that there are no realistic conditions (frequency range, stiffness of skeleton), where the behaviour of the impedance of air-saturated material matches the "in vacuum" one. The conclusion is that if the dynamical behaviour of a porous material is described by an infinite (impedance) approach, the "in vacuum" model cannot be used in place of Biot's model.

4. Modelling of finite-dimensional porous samples

In the previous section, the porous material has been considered as infinite in the lateral directions. The lateral dimensions have been taken into account through the area of the test

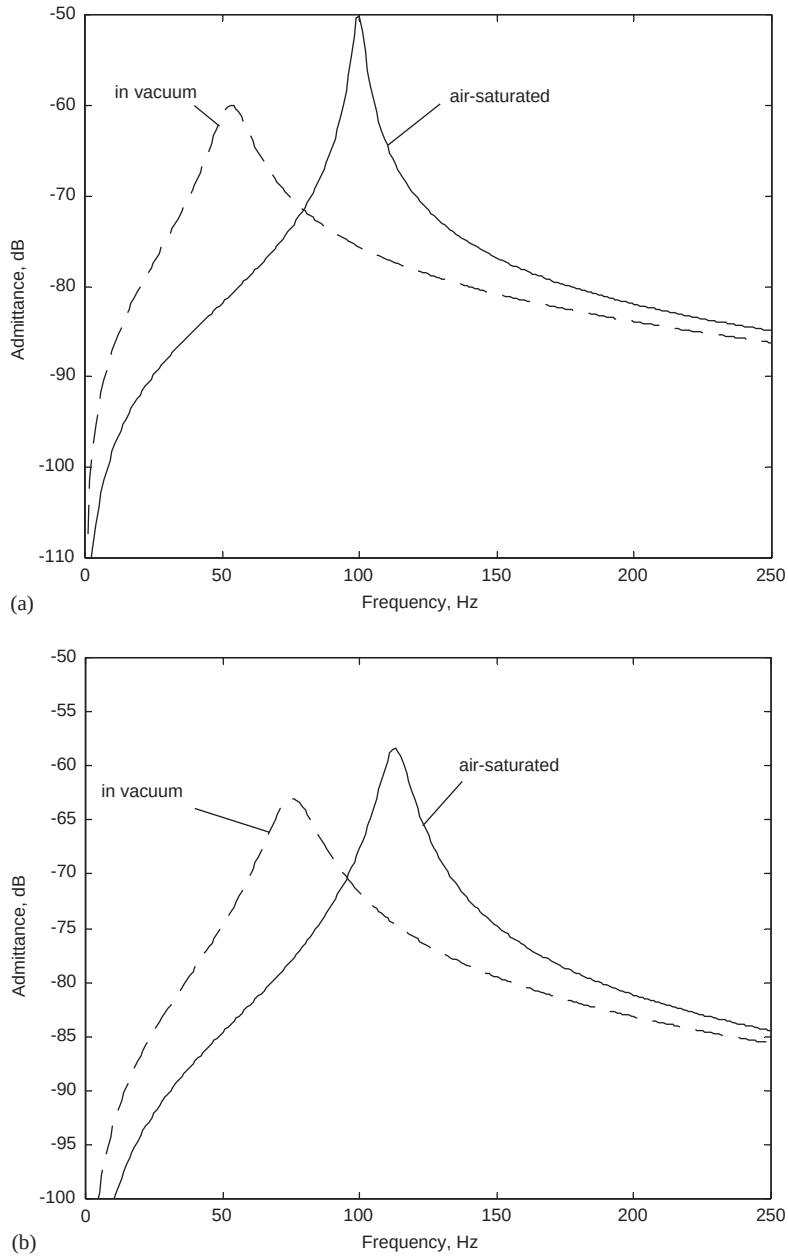

Fig. 9. Modulus of the admittance of porous material A with a mass atop obtained for low values of Young's modulus, (a) $E = 40\,\text{kPa}$, (b) $E = 80\,\text{kPa}$ and calculated using "air-saturated" and "in vacuum" models.

sample in order to find the mechanical impedance. However the characteristic impedance of the material was determined for infinite lateral dimensions. The next step of the comparison between the "air-saturated" material and the material "in vacuum" is done for a three-dimensional porous sample of fixed size. The poroelastic material is considered to have lateral boundary conditions

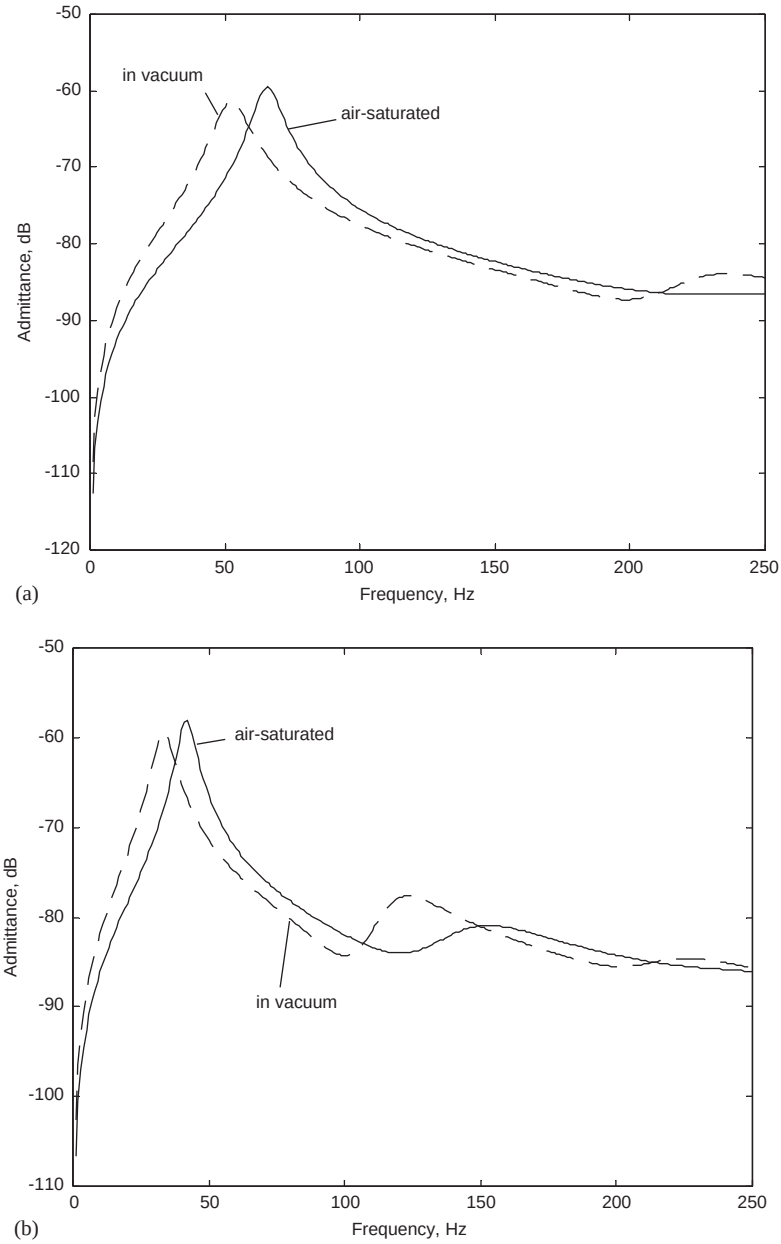

Fig. 10. Modulus of the admittance of porous material A with mass atop obtained for samples of large thickness, (a) thickness = 100 mm, (b) thickness = 200 mm and calculated using "air-saturated" and "in vacuum" models.

and the goal of this section is to find out how the lateral dimensions of the porous sample influence its behaviour. Table 1 gives the parameters of material A used in the numerical finite-element simulations. Considering that given set-ups used for the measurement of mechanical parameters (see Fig. 1) have free lateral sides, corresponding approximate boundary conditions

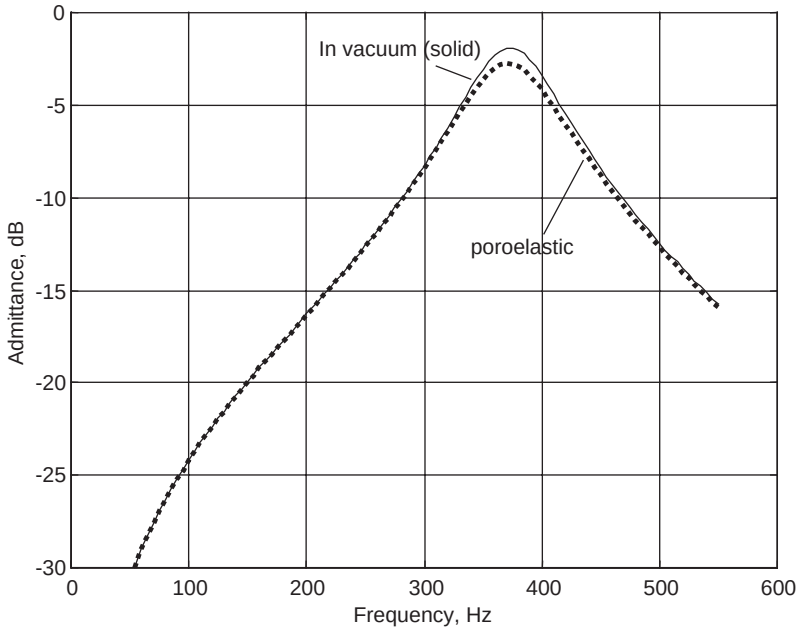

Fig. 11. Modulus of the admittance of a sample of material A with"free" boundary conditions calculated by a finite-element approach using "air-saturated" and "in vacuum" models.

consist in imposing interstitial pressure p to zero. In reality, the porous material can radiate in the surrounding medium so that the previous boundary condition is only approximate. The authors are not aware of any published work about the influence on the porous response of accounting exactly for the radiation condition. This is a topic which deserves the attention of researchers. Note that all the boundary conditions for the mixed poroelastic formulation are discussed in Ref. [19].

Fig. 11 shows the admittance modulus of a sample of material A with dimensions $0.041\,\mathrm{m} \times 0.041\,\mathrm{m} \times 0.027\,\mathrm{m}$ calculated using the "air-saturated" and the "in vacuum" models (poroelastic and solid elements, respectively). In both cases, a mesh of $2 \times 2 \times 4$ elements has been used in the numerical simulations. For other dimensions, the mesh has been adjusted in order to ensure the convergence of the solution. An excellent agreement is achieved between the two models. In particular, the resonance frequencies of both systems coincide. This frequency corresponds to the one calculated by Eq. (46). The picture also shows a slight difference of resonance amplitude between the two curves, which shows that the loss factor of the "air-saturated" material is higher than "in vacuum" one. The concordance of the resonance frequencies confirms the coincidence of Young's moduli and a slight difference of the resonance amplitude demonstrates a small difference of the loss factors. Similar numerical results have been obtained for other porous materials with the same dimensions.

Consider now the effect of the lateral dimensions of the porous sample on its "air-saturated" and "in vacuum" behaviours. The averaged admittance of the porous samples has then been calculated for multiple lateral dimensions. In order to synthesize the results, a convenient parameter which can be named "poroelastic shape factor" has been introduced. It is defined as the

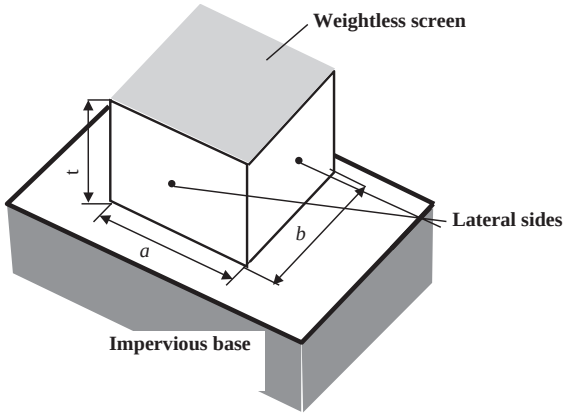

Fig. 12. Shape of test sample.

volume of the porous sample divided by the area of its lateral sides. For a test sample with a rectangular cross-section it is given by (see Fig. 12)

$$\frac{V}{S} = \frac{abt}{2(a+b)t}, \tag{47}$$

where a, b refer to the lateral dimensions and t denotes the thickness.

This parameter characterizes how small the test sample is, or, in other words, how strongly the boundary conditions influence the behaviour of the test sample as a whole. It is well-known that in resonant systems the resonance frequency characterizes the stiffness properties, in other words Young's modulus of the material. So, one can say that the difference (Δf) between the resonance frequencies in the case of the finite dimension sample with "free" lateral boundary conditions (poroelastic model) and in the case of the "in vacuum" model of the porous layer can be a measure of the well foundedness of using an "in vacuum" model instead of a poroelastic one. If the lateral dimensions of the sample were so large that the boundary conditions would not influence the behaviour of the sample, the difference Δf would be maximal and equal to the difference obtained between the "in vacuum" and the "poroelastic" infinite models. If the lateral dimensions of the sample were so small that the poroelastic sample would behave as an "in vacuum" one, the difference Δf would be zero. Note that Young's modulus is assumed frequency independent in the frequency band Δf.

Fig. 13 shows the above-mentioned parameter "Δf" versus V/S. It is seen that in the case of small magnitude of "poroelastic shape factor" (less than 0.02 m), the poroelastic model behaves as the viscoelastic one, then a transient zone is observed. Finally, in the case of large sample (V/S larger than 0.1 m), the same resonance frequency as in the case of the infinite approach is obtained.

Following the steps of the analytical impedance approach, the next phase is to investigate the behaviour of the finite-dimension porous sample as a function of the frequency zone where the resonance lies. In other words, does the criterion $V/S < 0.02$ m depend on the frequency range where the resonance takes place? Consider first the case where the resonance occurs at low frequencies. This behaviour has been achieved by adding a mass atop material A. The mass has

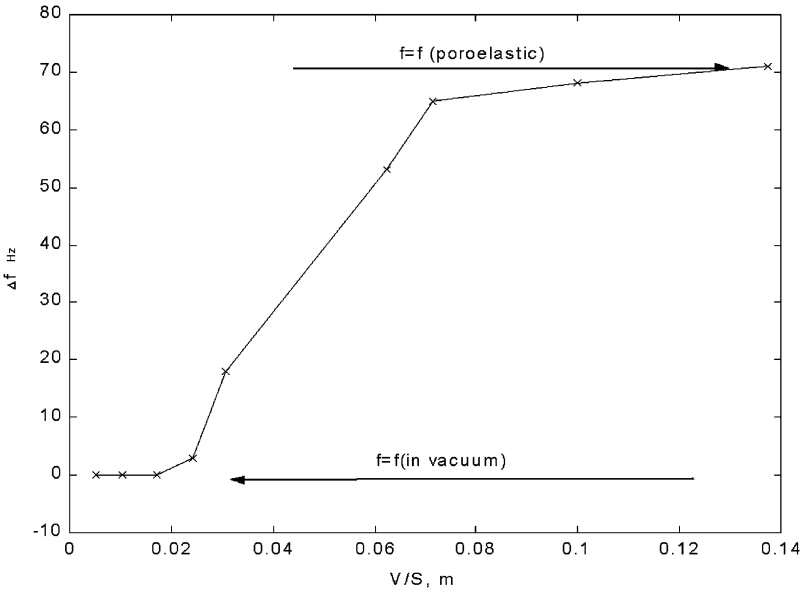

Fig. 13. Effect of the V/S parameter on "Δf" for material A.

been modelled by a layer of "septum" that is an additional mass without any stiffness (density and thickness equal to 7800 kg/m^3 and 1.66 mm, respectively). Fig. 14 shows the corresponding admittance modulus. A picture resembling Fig. 11 is obtained but the resonance frequency is lower (around 100 Hz instead of 372 Hz). The resonance frequencies of the "air-saturated" and "in vacuum" states of the material coincide and a slight difference in resonance amplitude is observed. Fig. 15 shows "Δf" versus V/S for this low-frequency configuration. The comparison between Figs. 13 and 15 shows that the reduction of the resonance frequency does not change the type of behaviour. Thus, the coincidence of resonance frequencies between "air-saturated" and "in vacuum" conditions is also observed below a limiting value of V/S equal to 0.02 m.

The behaviour of the porous sample in the high-frequency range has been examined just by increasing the porous layer Young's modulus. Table 3 presents the comparison between "air-saturated" and "in vacuum" resonance frequencies of the system. This simulation has been carried out for "small" dimensions of sample corresponding to $V/S = 0.017$ m. The increase of Young's modulus and, consequently the increase of resonance frequencies, does not lead to any difference between "air-saturated" and "in vacuum" resonance frequencies. The numerical analysis of Biot's and "in vacuum" models of the porous sample of finite dimension exhibit one criterion based on the shape factor V/S, which tells one when the latter can be used in place of the former. For the investigated cases, Biot's poroelastic and "in vacuum" models behave in the same way for "small" samples characterized by $V/S < 0.02$ m. This effect can be explained by the small value of the interstitial pressure in the pores imposed by the lateral boundary conditions. Indeed, the porous material is modelled as having "free" boundary conditions. This kind of boundary condition consists of setting the interstitial pressure to 0 at the boundary nodes [19]. This is only approximate since the acoustic radiation of the lateral sides of the sample in the outer medium is

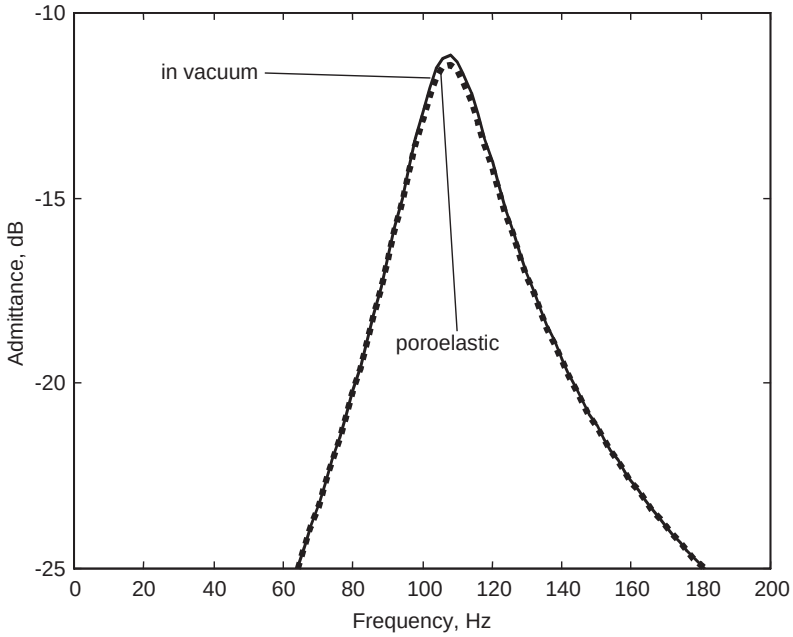

Fig. 14. Modulus of the admittance of a sample of material A with"free" boundary conditions with a mass atop calculated by a finite-element approach using "air-saturated" and "in vacuum" models.

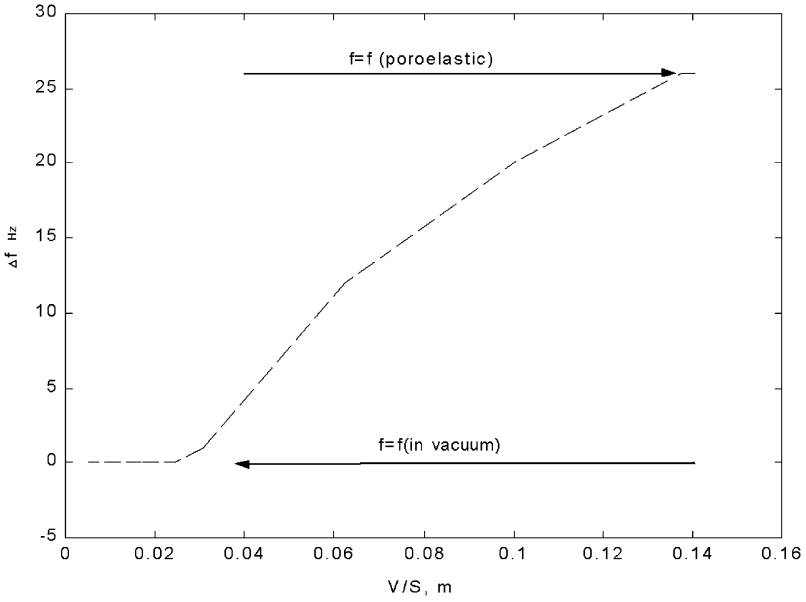

Fig. 15. Effect of the V/S parameter on "Δf" for material A with a mass atop.

Table 3
Effect of the increase of Young's modulus on the resonance frequencies—Material A

No.	Young's modulus (kPa)	Resonance frequency (Hz)	
		"In vacuum"	Poroelastic
1	170	372	372
2	250	453	447
3	300	495	491
4	400	572	568
5	500	640	635

neglected. Given the smallness of the samples, the interstitial pressure is uniform and almost zero so that the compressibility of air contained in the pores does not influence the parameters of the resonance and that is why the resonance frequency is completely determined by Young's modulus of skeleton. In other words, for a real material the air contained in the pores is not constrained and can escape the pores thereby not modifying the compressibility of the sample.

The resonance behaviour of the sample of the porous material allowed one to estimate its stiffness or its Young's modulus. Another important parameter related to the damping properties of the porous skeleton is the loss factor (η). In the previous figures, the width of the resonance curve and the amplitude at resonance are not the same for poroelastic and viscoelastic models, which means that the loss factor is not the same either. It is known that the total dissipated power in Biot's poroelastic model is the sum of three parts: the power dissipated in the skeleton, the power dissipated through viscous effects, and the power dissipated through compressibility effects. Fig. 16 displays the ratio of these three types of dissipated powers as a percentage of the total dissipated power per unit volume, calculated by a finite element approach. As V/S decreases from 0.14 to 0.03 m, the structural part (together with the viscous part) of the dissipated power decreases (the compressibility effects being negligible for this configuration). As the "poroelastic shape factor" decreases from 0.03 to 0 m, the viscous part of the dissipated power reduces dramatically, and the structural part increases very fast. For example, if $V/S = 0.0095$ (lateral size equal to 0.038×0.038 mm), 97% of the total dissipated energy is dissipated in the skeleton and one can observe the viscoelastic behaviour of the porous sample. The admittance of this configuration is shown in Fig. 17. A good agreement between both resonance curves ("air-saturated" and "in vacuum") confirms the "in vacuum" behaviour of an "air-saturated" sample of the porous material. This allows one to be confident in the estimate of its stiffness (Young's modulus) together with its damping properties (loss factor). Summarizing the obtained results one can say that the "in vacuum" approach can be applied to the poroelastic media in order to assess Young's modulus and loss factor if the "poroelastic shape factor" is less than 0.02 m. The above-mentioned conclusions have been obtained in the case of a "resistive" porous material (45 000 $\mathrm{Nm^{-4}s}$). One can wonder if the same value of the "poroelastic shape factor" is valid for a low-resistivity porous medium.

Two real low-resistivity materials have been numerically analyzed in order to investigate this question. Material C has very big dimensions of pores and, consequently, has a very low air flow resistivity (240 $\mathrm{Nm^{-4}s}$). Material D is typically used in industrial air conditioning systems and has an air flow resistivity equal to 3500 $\mathrm{Nm^{-4}s}$. For confidentiality reasons the materials properties

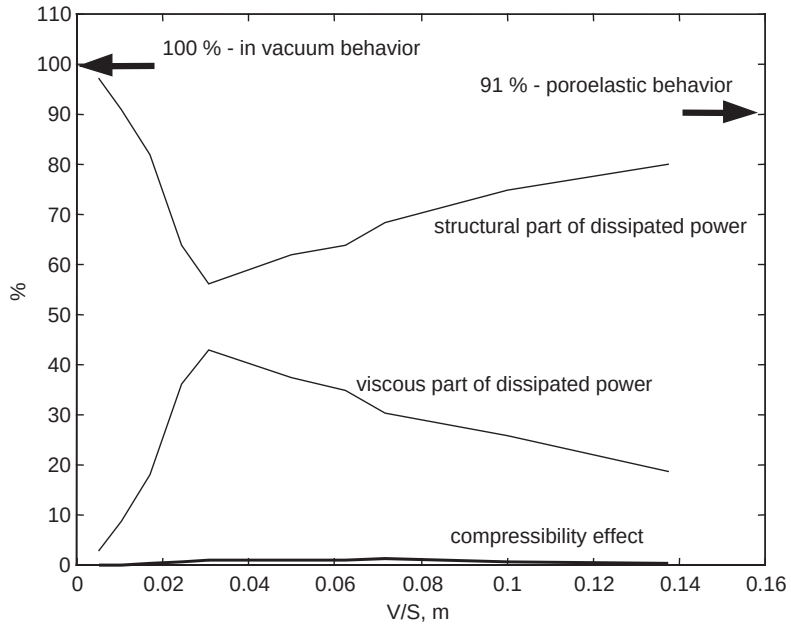

Fig. 16. Percentage of the total injected power dissipated by structural, viscous and compressibility effects versus V/S parameter—case of material A.

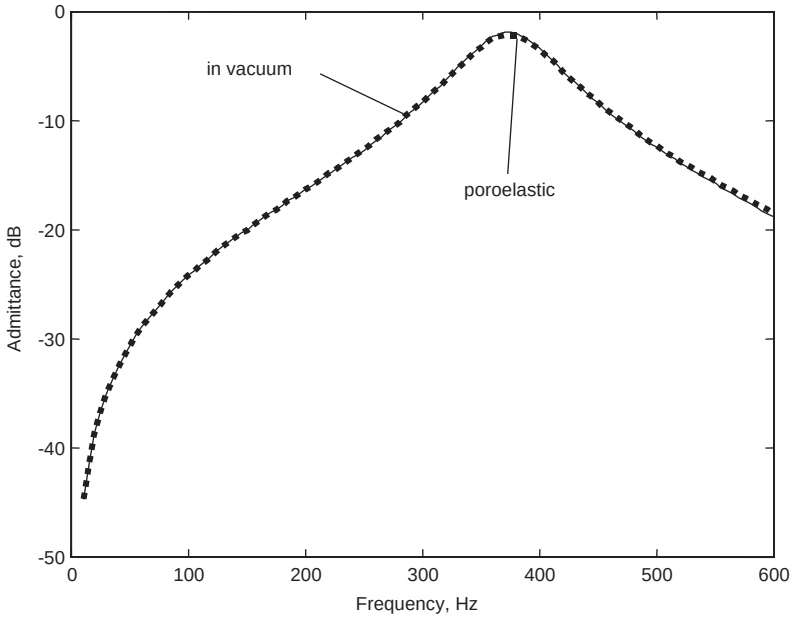

Fig. 17. Modulus of the admittance of a sample of material A with "free" boundary conditions, dimensions (0.038×0.038 mm) and a mass atop calculated by a finite-element approach using "air-saturated" and "in vacuum" models.

cannot be provided in this paper. Fig. 18 shows the powers dissipated by the three effects for material C as a percentage of the total dissipated power per unit volume, calculated by a finite-element approach. One can observe that 97% of the total power dissipated by skeleton is obtained in the case of $V/S = 0.1$ m, but material D has the same percentage of structural dissipated energy if V/S is equal to 0.03. At the same time, the finite-element simulation made for highly resistive material E (air flow resistivity of 60,000 Nm^{-4} s) indicates that this percentage is achieved for V/S equal to 0.0065 m. Fig. 19 displays the V/S parameter obtained for 97% of total power dissipated by skeleton as a function of the air flow resistivity. This figure reveals that as the flow resistivity decreases, the limiting "poroelastic shape factor" increases. In other words the measurements of mechanical parameters of low-resistivity porous materials can be accomplished using bigger test samples than for higher-resistivity materials.

For square cross-section samples with a side a, Eq. (47) reduces to $a/4$, which means that for these samples the thickness does not influence the magnitude of the "poroelastic shape factor". Note that in previous simulations the thickness of the porous samples has been kept constant to a value of 28 mm. It is now interesting to investigate the influence of the thickness on the limiting value of the V/S parameter. Fig. 20 displays the V/S parameter for 97% of the total power dissipated by skeleton as a function of the thickness of the sample for materials A and D. One can see a slight augmentation of this limit as the thickness increases but these results indicate a rather a weak dependence. Indeed, a multiplication of thickness by seven (from 7 to 50 mm) only induces

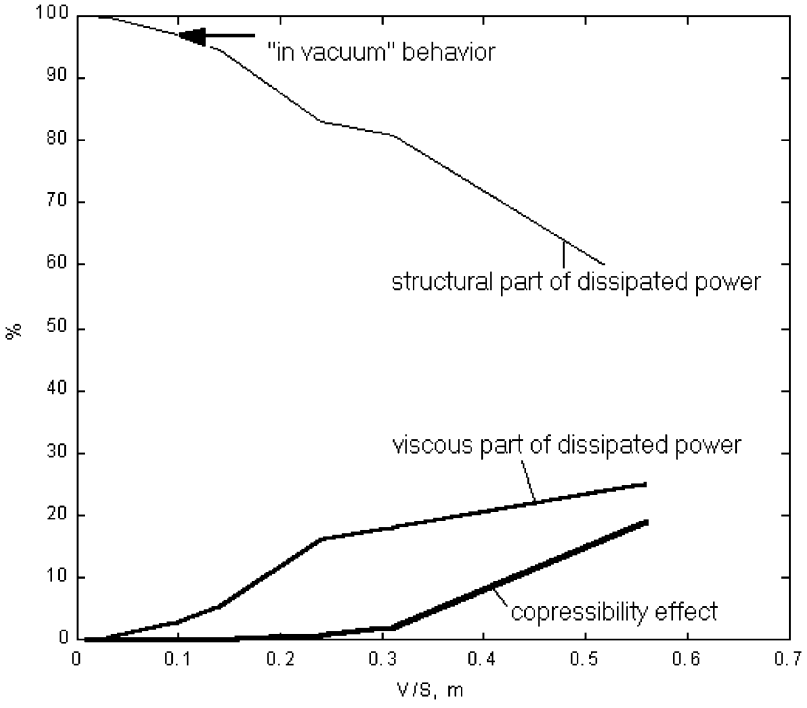

Fig. 18. Percentage of the total injected power dissipated by structural, viscous and compressibility effects versus V/S parameter - case of material C.

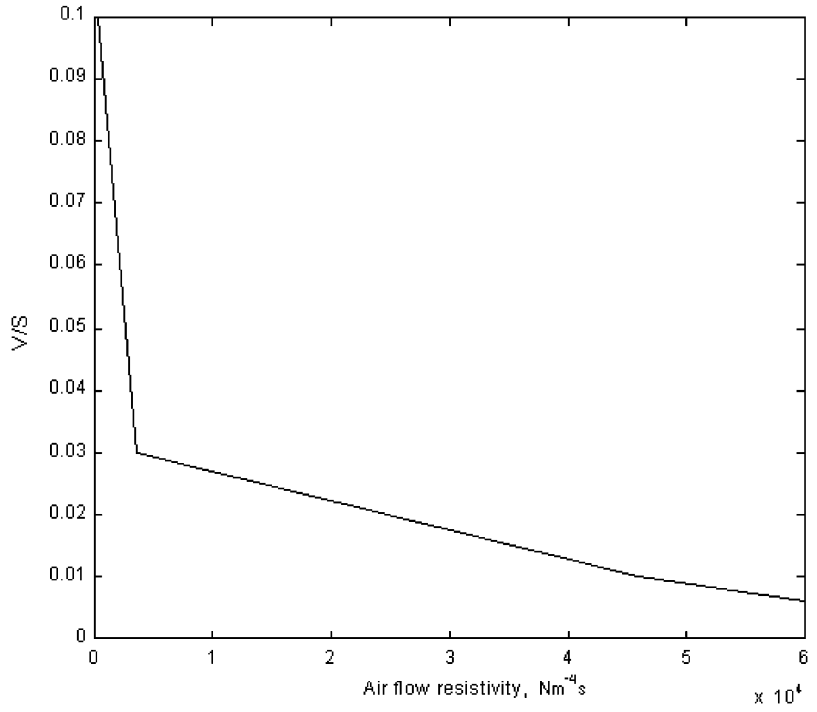

Fig. 19. Effect of the air flow resistivity on the limiting value of V/S parameter.

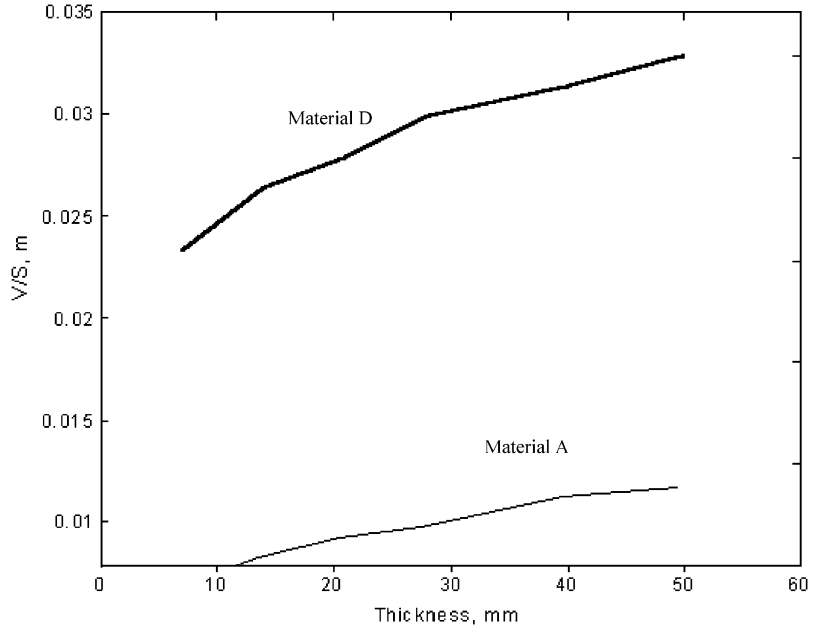

Fig. 20. Effect of the sample thickness on the limiting value V/S parameter.

a multiplication of the V/S parameter by 1.7. The observations derived from Fig. 20 indicate that the dependence of the limiting V/S parameter on the thickness is weak in comparison with air flow resistivity.

5. Conclusions

The purpose of this work was to investigate the conditions when a mechanically excited porous material exhibits an "in vacuum" behaviour, that is when its response is not influenced by its fluid phase and completely determined by the parameters of its solid phase. In other words, this paper examined the conditions under which "in vacuum" and "air-saturated" Biot's poroelastic models match. This study is indeed very useful to develop a correct measurement method for complex Young's modulus of porous skeleton. Impedance models of poroelastic "air-saturated" and "in vacuum" materials backed by an impervious rigid wall for the case of mechanical excitation have been first presented. The results based on these models show that there is no frequency range where the impedance of the porous material "in vacuum" and the "air-saturated" one coincide. In other words, poroelastic materials modelled by an impedance analytical model based on Biot's theory do not exhibit an "in vacuum" behaviour in their "normal" conditions. This simple model seems therefore inappropriate to estimate mechanical parameters of porous materials. A numerical model of the porous material accounting for finite dimension samples has been proposed to circumvent this issue. A "poroelastic shape factor" has been defined as the ratio of the volume to the area of the lateral sides of the porous sample considered as having free lateral boundary conditions. A finite-element analysis allowed one to establish limiting values of the poroelastic shape factor below which 97% of the total power in the porous medium is dissipated in the skeleton and the "in vacuum" and "air-saturated" models yield the same impedance. A possible explanation for this is that the air compressibility does not affect the behaviour of the skeleton because of the "free" lateral boundary conditions of the sample. Its dynamic behaviour is then completely determined by the complex Young's modulus of the skeleton. This conclusion has been verified in a rather wide frequency range, up to 650 Hz by analyzing materials with different Young's modulus magnitudes. It has been shown that the limiting values of the poroelastic shape factor depend on the flow resistivity and the thickness of the tested samples. In particular, an increase of this limit is achieved as the flow resistivity decreases and as the thickness increases.

Acknowledgements

This research was supported by Region Rhône-Alpes in the framework of research project IMPACT.

References

[1] A. Cragg, A finite element model for rigid porous absorbing materials, *Journal of Sound and Vibration* 61 (1978) 101–111.

[2] J.P. Coyette, H. Wynendaele, A finite element model for predicting the acoustical transmission characteristics of layered structures, in: R.J. Bernhard, J.S. Bolton (Eds.), *Proceedings of Inter-Noise' 95*, Newport Beach, CA, 1995, pp. 1279–1282.
[3] R. Panneton, N. Atalla, Numerical prediction of sound transmission through multilayer systems with isotropic poroelastic materials, *Journal of the Acoustical Society of America* 100 (1) (1996) 346–354.
[4] Y.J. Kang, J.S. Bolton, A finite element model for sound transmission through foam-lined double-panel structure, *Journal of the Acoustical Society of America* 99 (1996) 2755–2765.
[5] N. Atalla, R. Panneton, P. Debergue, A mixed displacement–pressure formulation for poroelasic materials, *Journal of the Acoustical Society of America* 104 (3) (1998) 1444–1452.
[6] M. Melon, Caractérisation de Matériaux Poreux par Ultrasons de Basses Fréquences (20–500 kHz), Ph.D. Dissertation, Univ. Du Maine, Le Mans, France, 1996.
[7] J. Tran-Van, X. Olny, F.C. Sgard, Y. Gervais, Global inverse methods for determine the acoustical parameters of anisotropic porous materials, *Proceedings of 17th International Congress on Acoustics*, Rome, 2001.
[8] R. Panneton, X. Olny, Analytical solutions for the characterization of the tortuosity and viscous characteristic length of porous media, Journal of the Acoustical Society of America, 2002, submitted.
[9] J.F. Allard, G. Jansens, G. Vermeir, W. Lauriks, Frame-borne surface waves in air-saturated porous media, *Journal of the Acoustical Society of America* 111 (2) (2002) 690–696.
[10] B. Brouard, M. Etchessahar, S. Sahraoui, Détermination expérimentale du module de rigidité en flexion d'une plaque de poreux aux basses fréquences, *Canadian Acoustics* 28 (3) (2000) 78–79.
[11] B.H. Song, J.S. Bolton, Y.J. Kang, Effect of circumferential edge constant on the acoustical properties of glass fiber materials, *Journal of the Acoustical Society of America* 110(6) (2001) 2902–2916.
[12] H.R. Tshudi, The development of new material characterization methods in order to achieve a better treatment optimization. Seventh UNIKELLER Conference, 1981.
[13] G. Lee, Resonance apparatus for damping measurements, *Metallurgical and Materials Transactions A* 26A (1995) 2819–2823.
[14] T. Pritz, Transfer function method for investigation of the complex modulus of acoustic materials: spring-like specimen, *Journal of Sound and Vibration* 72 (3) (1980) 317–341.
[15] E. Mariez, S. Sahraoui, J.F. Allard, Elastic constants of polyurethane foam's skeleton for Biot model, in: F.A. Hill, R. Lawrence (Eds.), *Proceedings of Inter-Noise' 96*, Liverpool, pp. 951–954.
[16] C. Langlois, R. Panneton, N. Atalla, Polynomial relations for quasi-static mechanical characterization of isotropic poroelastic materials, *Journal of the Acoustical Society of America* 110 (6) (2001) 3032–3040.
[17] J.F. Allard, Propagation of Sound in Porous Media: Modeling Sound Absorbing Materials, Elsevier, New York, 1993.
[18] MNS/NOVA™, version 1.0 http://www.mecanum.com.
[19] P. Debergue, R. Panneton, N. Atalla, Boundary conditions for the weak formulation of the mixed (*u*,*p*) mixed poroelasticity problem, *Journal of the Acoustical Society of America* 106 (5) (1999) 2383–2390.